



HAL
open science

Three-dimensional capillary force assembly: Fabrication of white light emitters

Julien Cordeiro, Olivier Lecarme, Guilherme Osvaldo Dias, David Peyrade

► **To cite this version:**

Julien Cordeiro, Olivier Lecarme, Guilherme Osvaldo Dias, David Peyrade. Three-dimensional capillary force assembly: Fabrication of white light emitters. *Journal of Vacuum Science & Technology B, Nanotechnology and Microelectronics*, 2012, 30 (6), pp.06F203-1. <10.1116/1.4764090>. <hal-00777320>

HAL Id: hal-00777320

<https://hal.science/hal-00777320v1>

Submitted on 21 Dec 2022

HAL is a multi-disciplinary open access archive for the deposit and dissemination of scientific research documents, whether they are published or not. The documents may come from teaching and research institutions in France or abroad, or from public or private research centers.

L'archive ouverte pluridisciplinaire **HAL**, est destinée au dépôt et à la diffusion de documents scientifiques de niveau recherche, publiés ou non, émanant des établissements d'enseignement et de recherche français ou étrangers, des laboratoires publics ou privés.



HAL Authorization

Three-dimensional capillary force assembly: Fabrication of white light emitters

Julien Cordeiro, Olivier Lecarme, Guilherme Osvaldo Dias, and David Peyrade^{a)}
LTM-CNRS-UJF-Grenoble INP, 17 rue des Martyrs 38054 Grenoble, France

(Received 27 June 2012; accepted 10 October 2012; published 25 October 2012)

This work uses convective assisted capillary force assembly from a collection of 100 nm fluorescent polystyrene nanoparticles to fabricate 4 μm wide and 1 μm high localized light-emitting superstructures. Large scale superstructures of about 10 000 particles are transferred on free silicon surfaces by microcontact printing. Optical characterization reveals that these sources emit polychromatic visible light from 400 to 800 nm equivalent to a white spectrum. Finally, single objects are studied to characterize the spatial distribution of the emitted color. © 2012 American Vacuum Society. [<http://dx.doi.org/10.1116/1.4764090>]

I. INTRODUCTION

The production of white light emitters is very well controlled by various techniques. Such techniques are, for example, the optical mixing of red, green, and blue (RGB) monochromatic light-emitting diodes (LEDs),¹ or the spectral down conversion with phosphor-coated LEDs.² These light sources are only mainly used in millimeter or centimeter-sized systems. However, some fields of physics, such as integrated optics, require micrometer-sized sources for the development of photonic circuits. It is therefore necessary to resort to less conventional methods.

Thus many alternative techniques have been proposed the last few years, mainly based on the use of doped polymers,^{3,4} quantum dots^{5,6} or nanowires.^{7,8} But also colloids can be used to make light sources. Recently, fluorescent particles were assembled into multilayers on a GaN light-emitting diode to produce polychromatic light sources.^{9–11} However, to achieve deterministically localized sources on “optical chips,” a precise control of the position of the nanoparticles is required. Among others this can be interesting for coupling the light sources with integrated optical components as waveguides. The localization of the nanoparticles can be realized by different methods based on optical forces,^{12,13} electrostatic,¹⁴ or even dewetting.^{15–18} The latter has already proven its efficiency in coupling colloidal light sources with optical waveguides.¹⁹

In this work, a fabrication process based on convective assisted capillary force assembly (CA-CFA) and microcontact printing is presented for the conception of colloidal white light emitters with micrometric size and deterministic localization. Fluorescent particles-based superstructures are optically characterized and their fluorescence spectrum is measured. Finally, the spatial distribution of the emitted light from a single object is discussed.

II. FABRICATION OF WHITE LIGHT EMITTERS

A. CA-CFA

The movement of particles in a colloidal suspension is controlled by the Brownian motion due to thermal agitation. To overcome this random movement, an experimental setup,

described in details in previous work,²⁰ named CA-CFA has been developed. It is based on controlling the evaporation of a colloidal droplet on a patterned surface in a microfluidic cell. The environmental parameters, such as temperature (T) (from 25 to 55 °C) and air suction flow (Q) (from 10 to 200 ml/min), are precisely adjusted in order to deterministically position a large variety of particles in terms of material, size, and shape. Thus, it was already possible to assemble metallic,^{21,22} dielectric,¹⁹ or organic²³ colloids with sizes from 50 nm to 10 μm for plasmonics, integrated optics, and biological applications, respectively. The assembly process is achieved via two forces. First, the hydrodynamic force, created by the convection flows, that drags the colloids at the triple interface (solid–liquid–vapor). Second, the capillary immersion force that pushes them into the patterns of the sample.

B. Fabrication process

Fluorescent nanoparticles form the building blocks for the fabrication of micrometric clusters that emit light. Those clusters are named particles super structures (PSS) and require a series of elaboration steps. First, a silicon master is fabricated by optical lithography using a SU8 2002 negative photoresist (MicroChem) followed by dry etching (HBr, Cl, O₂ plasma). The depth of the patterns can be adjusted to control the number of particle layers constituting the PSS. In the following, the pattern thickness is fixed at 1.3 μm . The residual resist is then removed by O₂ plasma [Fig. 1(b)(1)].

Second, polydimethylsiloxane (PDMS) is spin-coated at 500 rpm on the silicon master and baked at 110 °C for 1 h to ensure a 130 μm thick stamp [Fig. 1(b)(2)], which is then removed from the master [Fig. 1(b)(3)] and used as assembly surface for the CA-CFA step.

Simultaneously, a colloidal solution [Fig. 1(a)] is prepared with 100 nm fluorescent polystyrene (PS) nanoparticles. Red, green, and blue fluorescent nanoparticles are mixed with a volume ratio of 13:10:6 and diluted by 20 in deionised water. This ratio has been determined beforehand by studying the chromaticity diagram. To reduce the contact angle between the solution and the PDMS surface, which will allow the colloid assembly, the initial surfactant is removed by centrifugation and replaced by Triton X-100 at

^{a)}Electronic mail: david.peyrade@cea.fr

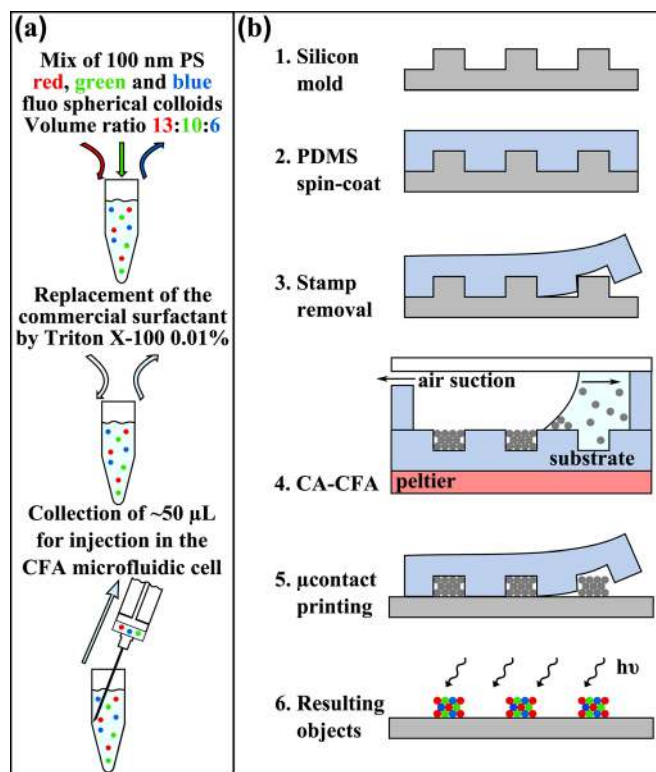


Fig. 1. (Color online) (a) Preparation of the multifluorescent colloidal solution. (b) Fabrication process of the PSS.

0.01% in mass. The initial contact angle of 110° then passes to 40° .

The PDMS sample is placed under a microfluidic system composed of a PDMS spacer with a cover glass slide. This stack is then deposited on a Peltier controller (T) and linked to a peristaltic pump (Q). A small amount of the solution is collected and injected to partially fill the microfluidic cell [Fig. 1(b)(4)]. The colloids are assembled at 45°C and the vapor saturated air in the microfluidic cell is sucked out at a flow rate of 10 ml/min. To ensure the total filling of the patterns and thus facilitate the transfer of the structures, the CFA step is repeated three times on the same sample.

Finally, the particle superstructures are transferred by microcontact printing [Fig. 1(b)(5)] on a substrate of higher surface energy ($>150\text{ mN/m}$ for glass and silicon) than PDMS (30 mN/m). The PDMS stamp is put up-side down onto the sample and pressed ($\sim 900\text{ kPa}$) for about 10 s against the host surface which is heated at 100°C . The pressure applied during the transfer ensures a good contact between the particles and the host surface. The PDMS is then peeled off and cooled down at room temperature.

Scanning electron microscope (Zeiss Ultra Plus) observations revealed that, with this process, networks of three-dimensional objects ($1\ \mu\text{m}$ high and $4\ \mu\text{m}$ wide) can be built [Fig. 2(a)]. Examination of a single object confirms that the integrity of the structure is preserved during the transfer step. The shape is well defined and the faces are flat without any deformations [Fig. 2(b)]. These objects are composed of about $12\,000 \pm 1\%$ particles of 100 nm diameter arranged in 15 layers [Fig. 2(c)]. The volume of the PSS can be tuned to

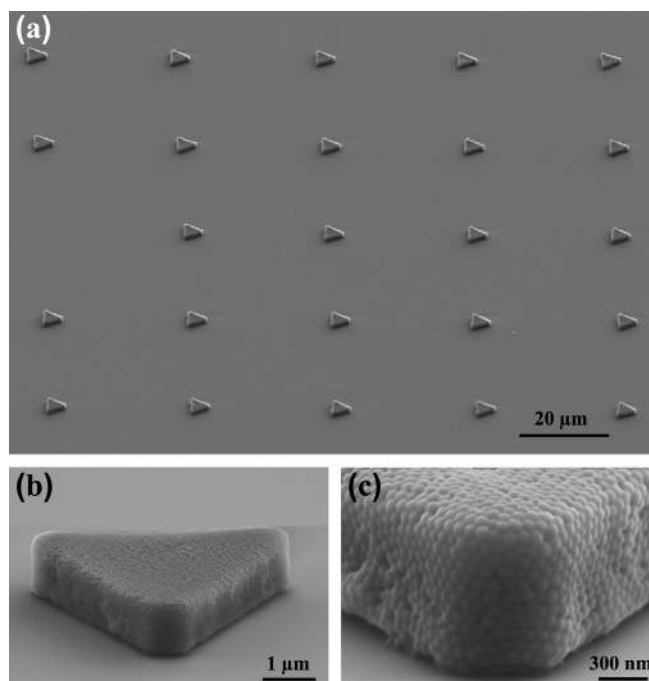


Fig. 2. SEM micrographs of the transferred triangular PSS: (a) large scale view, (b) zoom on a single object, (c) details of the crystalline arrangement.

vary from 10^{-3} to $10^3\ \mu\text{m}^3$ with a pitch down to 100 nm (for an efficient assembly). For this study, the PSS volume has been fixed to $7\ \mu\text{m}^3$ with $25\ \mu\text{m}$ distance between each object. Thereby, the PSS are composed of enough particles to statistically preserve the RGB ratio and are sufficiently distant from each other to allow the study of individual objects. Due to their spheric shape and the self-assembly process, the nanoparticles form hexagonal close-packed opal structures comparable to those of the photonic crystals.

III. OPTICAL CHARACTERIZATION

A. Experimental setup

The white light emitters are optically characterized with an inverted fluorescence microscope (Zeiss AxioObserver Z1m). The sample is illuminated with a UV light at 365 nm and the emitted light is collected at its surface with a $100\times$ objective [Fig. 3(a)]. The optical response of the PSS can be studied using different emission filters [Fig. 3(b)].

For the fluorescent spectrum measurement, the emitted light is transmitted through a multimode optical fiber to a Peltier cooled spectrometer (OceanOptics QE65000). The fiber is chosen with a core diameter of $400\ \mu\text{m}$ to collect the light from an area of $4\ \mu\text{m}$ and thus ensures the study of a single structure.

B. Results and discussion

The principle of fluorescent white light emission consists in using a unique light source to generate a broadband emission covering the visible light spectrum. In our case, a UV source is used to excite PS nanoparticles doped with different fluorescent dyes. First, the blue dye-doped nanospheres with an absorption wavelength at 365 nm and an emission in the blue range are excited with the UV. One part of the

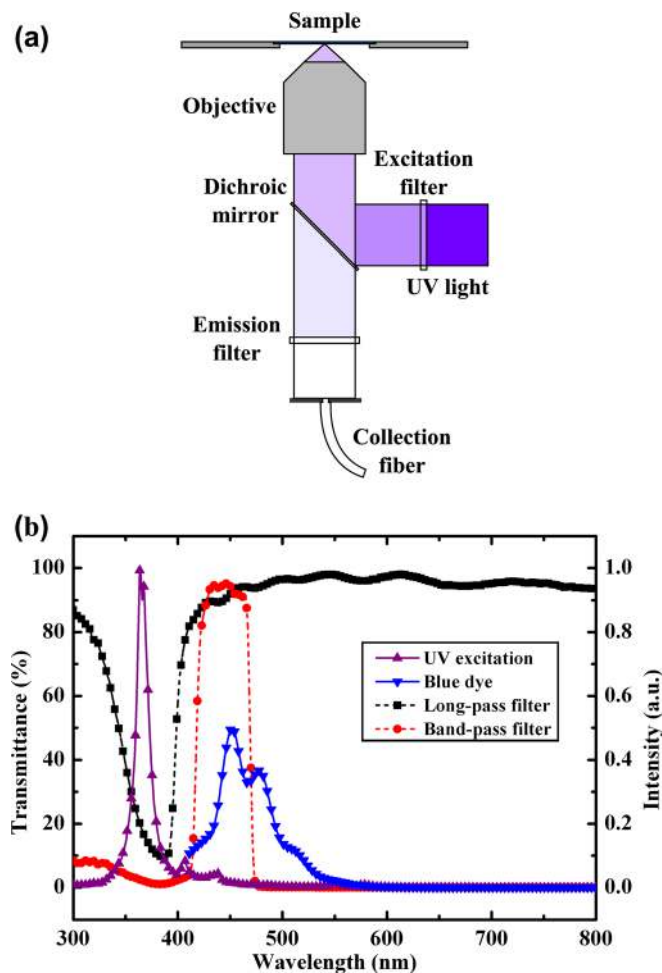


Fig. 3. (Color online) (a) Schematic view of the optical experimental setup. (b) Example of the spectrum obtained for blue dyes (blue curve) with a 365 nm illumination (violet curve); Emission filters used for blue and white light collection plotted in black and red, respectively.

emitted light is diffused in the far field while the other part is reabsorbed by the green dye-doped nanospheres at 468 nm. These particles also absorb the UV light and emit in the green range. Finally, the red-dye doped nanospheres are excited at 542 nm by the UV light and the previous emissions (from the blue and green particles) and emit in the red range. The sum of the blue, green, and red far-field contributions should result in a polychromatic emission.

The color of the light emitted from the colloidal structures is investigated with different emission filters. First, a band-pass filter at 450 ± 18 nm is used to reveal the presence of the blue colloids. Then, this filter is replaced by a band-pass filter at 490 ± 20 nm to observe the contribution of the green particles. Finally, the red emission is detected with a band-pass filter at 630 ± 40 nm. As expected, the superposition of these different contributions results in a white light emission that can be observed using a long-pass filter at 400 nm [Fig. 4(b)].

To study the spectral distribution of this emitted white light, localized spectroscopy is carried out on the triangular transferred PSS. The spectrum is acquired and compared to those of the individual dye-doped nanospheres. As shown in

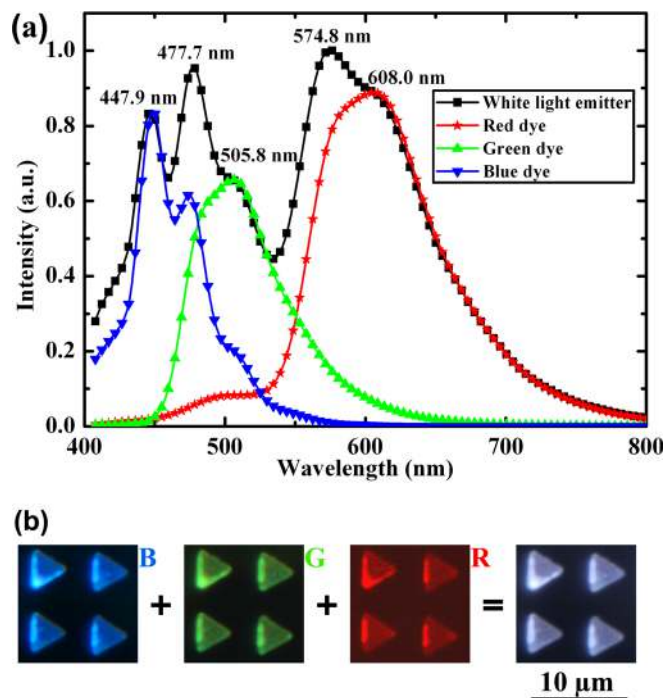


Fig. 4. (Color online) (a) Localized, normalized fluorescence spectra acquired on dry droplets of unmixed individual particles illuminated with UV (blue, green, and red curve) and on the PSS (black curve). (b) Fluorescent micrographs of triangular PSS obtained with band-pass filters (blue, green, red) and long-pass filter (white).

Fig. 4(a), the resulting spectrum covers the whole visible range (from 400 to 700 nm) and is composed of five fluorescent peaks. Those peaks correspond exactly to the emission of each individual encapsulated fluorescent dye. When measured individually, the unmixed blue nanospheres produce three peaks at 448, 478, and 506 nm, the green ones emit two peaks at 478 and 506 nm and the red nanospheres fluoresce also with two peaks at 575 and 608 nm. The white emission can be therefore described as a physiological white since it results from a superposition of the three primary colors (red, green, and blue) captured by the cones of the human eye, in contrast to a physical white that consists of a continuous emission of all the visible wavelengths as it is obtained with a black body. This implies that the spectrum of the white emission depends only on the used colors and therefore on the fluorescent dyes employed for the fabrication of the PSS. For this reason, it should be possible to tune the emitted color by adjusting the ratio of the red, green, and blue nanoparticles.

The measurement of the optical response is repeated on approximately ten structures to validate the potential of the CA-CFA technique to manufacture arrays of identical objects. The shape of the resulting spectra (position and ratio between the peaks) remains relatively unchanged from one object to another [Fig. 5(a)] which indicates that the high number of particles forming an object permits to statistically preserve the R:G:B ratio used for the assembly step.

Finally, we studied the spatial homogeneity of the light emitted by a single structure by replacing the 400 μ m optical fiber by a smaller core diameter fiber of 50 μ m. Thereby, it is

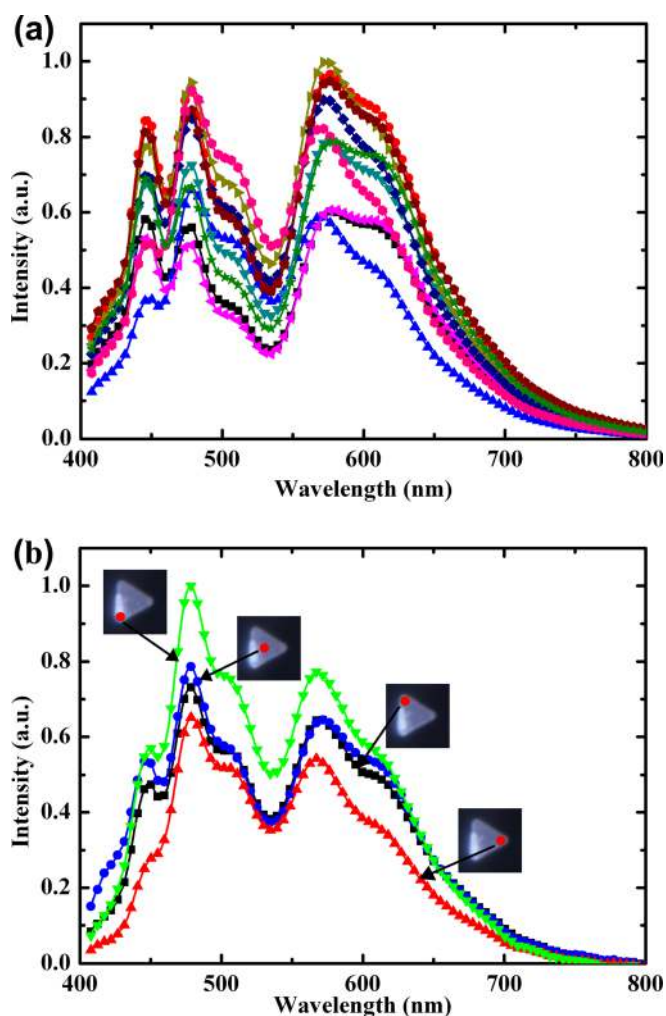


Fig. 5. (Color online) (a) Localized, normalized fluorescence spectra acquired on ten different triangular PSS. (b) Localized, normalized fluorescence spectra acquired on different regions of interest on the same object.

possible to collect the light coming from an area of 500 nm and so scan the surface of a single object. Four regions have been examined for the triangular PSS, the three corners and the middle of the structure. All the measured spectra consist of the same fluorescent peaks [Fig. 5(b)] that correspond to the peaks described previously. The fluctuation of the emitted intensity between the different regions of interest can be easily explained by a variation of the number of particles present in these areas. Thus, the most filled zones appear brighter, while those with a lack of particles appear darker. However, if the ratio between the different peaks of the white spectrum is measured, the result seems to be the same wherever the object is scanned. This means that the emitted color is uniformly distributed over the object and does not depend on where the structure is observed.

IV. CONCLUSIONS

A quick and complete fabrication process based on both Convective Assisted Capillary Force Assembly and micro-contact printing have been developed to build micrometric particle superstructures from 100 nm PS fluorescent colloidal

solution. This technique allows the fabrication of large scale networks ($1 \times 1 \text{ cm}^2$) of on-chip localized polychromatic light emitters on high surface energy substrates, as silicon or glass.

The optical characterization has revealed that the use of fluorescent nanoparticles (red, green, and blue) allows the emission of a polychromatic light due to the far-field superposition of the three colors. The measurement of the emitted spectrum by localized microspectroscopy on transferred objects has shown a continuous emission from 400 to 700 nm, consisting of five fluorescent peaks that can be assumed as a white light emission. Finally, the color has been studied in terms of spatial distribution. The spectra have highlighted the homogeneity of the light emitted by the different parts of a single structure.

Due to its versatility, the CA-CFA technique may offer the possibility to build different kinds of emitters in terms of shape and size and especially to tune the color of the emitted light by adjusting the ratio of the RGB fluorescent particles. Hence, the manufacture of ultra localized and high quality white sources could be considered. Moreover, the opportunity to transfer these structures on a wide variety of substrates suggests the coupling with other integrated optical components (as waveguides) in order to use them as sensors or characterization tools.

¹I. Moreno and U. Contreras, *Opt. Express* **15**, 3607 (2007).

²S. Nishiura, S. Tanabe, K. Fujioka, and Y. Fujimoto, *Opt. Mater.* **33**, 688 (2011).

³C. W. Seo and J. Y. Lee, *Thin Solid Films* **520**, 5075 (2012).

⁴H. T. Nicolai, A. Hof, and P. W. M. Blom, *Adv. Funct. Mater.* **22**, 2040 (2012).

⁵W. S. Song and H. Yang, *Chem. Mater.* **24**, 1961 (2012).

⁶T. E. Rosson, S. M. Claiborne, J. R. McBride, B. S. Stratton, and S. J. Rosenthal, *J. Am. Chem. Soc.* **134**, 8006 (2012).

⁷C. H. Chen, S. J. Chang, S. P. Chang, M. J. Li, I. C. Chen, T. J. Hsueh, A. D. Hsu, and C. L. Hsu, *J. Phys. Chem. C* **114**, 12422 (2010).

⁸Z. Yang, J. Xu, P. Wang, X. Zhuang, A. Pan, and L. Tong, *Nano Lett.* **11**, 5085 (2011).

⁹K. N. Hui, P. T. Lai, and H. W. Choi, *Opt. Express* **16**, 13 (2008).

¹⁰K. N. Hui, W. Y. Fu, W. N. Ng, C. H. Leung, P. T. Lai, K. K. Y. Wong, and H. W. Choi, *Nanotechnology* **19**, 355203 (2008).

¹¹K. N. Hui, W. N. Ng, C. H. Leung, P. T. Lai, and H. W. Choi, *Phys. Status Solidi C* **5**, 2201 (2008).

¹²S. Nedeve, A. S. Urban, A. A. Lutich, and J. Feldmann, *Nano Lett.* **11**, 5066 (2011).

¹³C. Renaut, J. Dellinger, B. Cluzel, T. Honegger, D. Peyrade, E. Picard, F. de Fornel, and E. Hadji, *Appl. Phys. Lett.* **100**, 101103 (2012).

¹⁴E. Palleau, N. M. Sangeetha, and L. Ressler, *Nanotechnology* **22**, 325603 (2011).

¹⁵Q. He, F. Sévéric, H. Hajjoul, Y. Viero, and A. Bancaud, *Langmuir* **27**, 6598 (2011).

¹⁶A. Merlin, J. B. Salmon, and J. Leng, *Soft Matter* **8**, 3526 (2012).

¹⁷D. Debuissou, V. Senez, and S. Arscott, *J. Micromech. Microeng.* **21**, 065011 (2011).

¹⁸M. J. Gordon and D. Peyrade, *Appl. Phys. Lett.* **89**, 053112 (2006).

¹⁹O. Lecarme, T. Pinedo Rivera, L. Arbez, T. Honegger, K. Berton, and D. Peyrade, *J. Vac. Sci. Technol. B* **28**, C6O11 (2010).

²⁰T. Pinedo Rivera, O. Lecarme, J. Hartmann, E. Rossitto, K. Berton, and D. Peyrade, *J. Vac. Sci. Technol. B* **26**, 2513 (2008).

²¹T. Pinedo Rivera, O. Lecarme, J. Hartmann, R. L. Inglebert, and D. Peyrade, *Microelectron. Eng.* **86**, 1089 (2009).

²²O. Lecarme, T. Pinedo Rivera, K. Berton, J. Berthier, and D. Peyrade, *Appl. Phys. Lett.* **98**, 083122 (2011).

²³N. Broguière, T. Pinedo Rivera, B. Pépin-Donat, A. Nicolas, and D. Peyrade, *Microelectron. Eng.* **88**, 1821 (2011).